

## UPCONVERSION AVALANCHE PROCESSES IN Ho<sup>3+</sup>-Yb<sup>3+</sup>:YLF CRYSTAL

E. OSIAC<sup>1</sup>, S. KÜCK<sup>2</sup>, I. SOKÓLSKA<sup>3</sup>, M. OSIAC<sup>4</sup>, G. HUBER<sup>5</sup>

<sup>1</sup> University of Medicine and Pharmacy of Craiova, str. Petru Rare no. 4, Craiova 1100 Romania,  
e-mail: e\_osiac@yahoo.com

<sup>2</sup> Physikalisch-Technische Bundesanstalt, Bundesallee 100, 38116 Braunschweig, Germany

<sup>3</sup> Not affiliated

<sup>4</sup> University of Craiova, str. A. I. Cuza no. 13, Craiova 1100, Romania

<sup>5</sup> Institut für Laser Physik, Universitaet Hamburg, Luruper Chaussee 149, 22761 Hamburg, Germany

(Received August 12, 2008)

*Abstract.* This paper analyses the upconversion avalanche mechanism under excitation around 750 nm and around 800–830 nm in the Ho<sup>3+</sup>, Yb<sup>3+</sup>:YLF system. Based on a rate equation model, a numerical simulation of the avalanche processes is provided.

*Key word:* avalanche process, Ho<sup>3+</sup> ions, Yb<sup>3+</sup> ions, YLF system, rate equation numerical simulation.

### 1. INTRODUCTION

In the last years one of the most studied rare-earth ions in order to search for upconversion processes is the Ho<sup>3+</sup>-ion [1–16]. From the point of view of upconversion processes the Ho<sup>3+</sup> ion offers some very interesting possibilities: it has a high lying green emitting level (<sup>5</sup>S<sub>2</sub>) and metastable levels (<sup>5</sup>I<sub>7</sub> and <sup>5</sup>I<sub>6</sub>), from where efficient infrared excited state absorption (ESA) processes can occur. Also many non-radiative energy transfer processes such as cross-relaxation or upconversion can help in building upconverted population.

The avalanche mechanism [17–19] denotes a particular type of upconversion. In such a process, weak ground state absorption (GSA) leads to a small population in an intermediate level, the so-called “reservoir level”, (Fig. 1). The ESA process from this reservoir level is very strong, thus bringing the excitation in the emitting level. An efficient feed back mechanism, e.g. cross relaxation (CR), connects the emitting level, the reservoir level and the ground level, thus enhancing efficiently the population in the reservoir level. There are several “signatures” of the avalanche mechanism: first, the pump power dependence in logarithmic scale of the

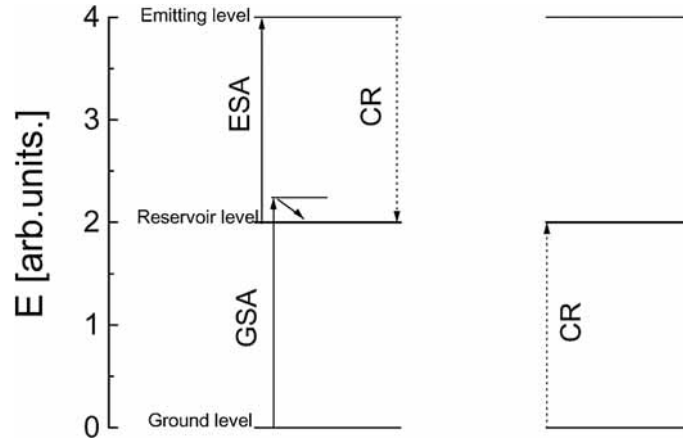


Fig. 1 – Avalanche mechanism.

upconverted emission shows a specific shape beginning with a slope of 2, then around a threshold value of the pump rate a powerful increase with a slope larger than 2 occurs, which is finally followed at high pump powers by a saturation behaviour. Also the temporal behavior of the upconverted emission under cw excitation depicts different shapes below and above the threshold value of the pump power. All these characteristics are extensively described in [17–19].

Efficient avalanche mechanisms were already reported in  $\text{Pr}^{3+}$  [20, 21],  $\text{Pr}^{3+}\text{-Yb}^{3+}$  [22, 23],  $\text{Tm}^{3+}$  [24, 25],  $\text{Nd}^{3+}$  [26, 27] and  $\text{Er}^{3+}$  doped systems [28]. In  $\text{Ho}^{3+}$ , green emission due to an avalanche mechanism was observed under 590 nm [29] and under 750 nm excitation in  $\text{Ho}^{3+}\text{:YLF}$  [7] and around 830 nm in  $\text{Ho}^{3+}$ ,  $\text{Yb}^{3+}\text{:YAlO}_3$  [9].

For a complete analysis of the process the ESA transitions of  $\text{Ho}^{3+}$  in the above mentioned spectral range were measured by standard probe and pump technique. Based on phase sensitive measurements the transitions originating from  $^5I_6$  around 750 nm were separated from the transitions originating from the  $^5I_7$  [30].

In order to make the avalanche mechanism more efficient we have codoped the  $\text{Ho}^{3+}\text{:YLiF}_4$  system with  $\text{Yb}^{3+}$ . The  $\text{Yb}^{3+}$ -ion is one of the most used sensitizer ions. Its configuration ( $f^{13}$ ) as a free ion has only two multiplets, namely  $^2F_{5/2}$  and  $^2F_{7/2}$ . It is very easily introduced in large concentrations in an appropriate crystalline matrix. A large concentration of  $\text{Yb}^{3+}$ -ions also assures a good homogeneity of the  $\text{Ho}^{3+}\text{-Yb}^{3+}$  system due to the energy migration process inside the  $\text{Yb}^{3+}$  ion system. Early studies of  $\text{Ho}^{3+}\text{-Yb}^{3+}$  systems [31–33] concentrated on the excitation in the  $\text{Yb}^{3+}$  ion in the 940–970 nm spectral region. Nevertheless, the possibility of realizing an upconversion laser using excitation in  $\text{Yb}^{3+}$  (940–970 nm) was proven to fail due to the strong  $\text{Ho}^{3+}\text{-Yb}^{3+}$  ( $^5S_2$ ,  $^2F_{7/2}$ )  $\rightarrow$  ( $^5I_6$ ,  $^2F_{5/2}$ ) cross-relaxation process [34].

## 2. RESULTS AND DISCUSSION

In the single Ho<sup>3+</sup>:YLF system the characteristics of the avalanche mechanism were observed under 750 nm excitation while in Ho<sup>3+</sup>:YAlO<sub>3</sub> using a 754 nm excitation only a looping mechanism was put into evidence [8]. The reason was proven to be a small efficiency of the cross-relaxation mechanisms that feed the reservoir level back. By introduction of the Yb<sup>3+</sup> ion it was demonstrated [9] that in Ho<sup>3+</sup>, Yb<sup>3+</sup>:YAlO<sub>3</sub> the avalanche mechanism under 754 nm excitation occurs. Therefore the introduction of Yb<sup>3+</sup> seems to be a promising solution to increase the efficiency of the avalanche mechanism also in the YLF crystal. Fig. 2 depicts the possible mechanisms in the Ho<sup>3+</sup>-Yb<sup>3+</sup> system leading to an upconversion avalanche mechanism under excitation around 750 nm.

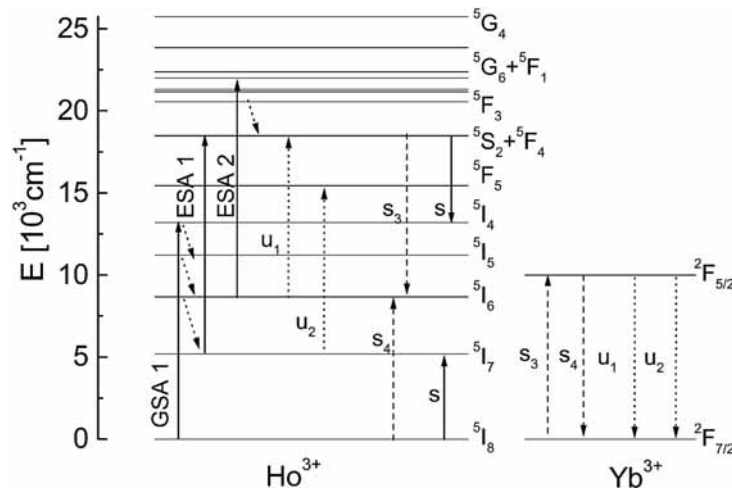


Fig. 2 – Energy levels of Ho<sup>3+</sup> and Yb<sup>3+</sup> ions and possible energy transfer processes in the Ho<sup>3+</sup>-Yb<sup>3+</sup> system.

The mechanism leading to the upconversion avalanche process in the Ho-Yb system under excitation around 750 nm starts (Fig. 2), as in the case of the single doped crystal, with the initial step represented by a weak ground state absorption (GSA1) followed by fast phonon deexcitation to the <sup>5</sup>I<sub>6</sub> and <sup>5</sup>I<sub>7</sub> levels from which ESA1 and ESA2 occur. Two cross-relaxation processes named *s* and *s*<sub>3</sub> affect the <sup>5</sup>S<sub>2</sub> population. The first process feeds directly the <sup>5</sup>I<sub>7</sub> level while the second process *s*<sub>3</sub> involves also Yb<sup>3+</sup>-ions and feeds in connection with process *s*<sub>4</sub> mainly the <sup>5</sup>I<sub>6</sub> level. From the <sup>5</sup>I<sub>6</sub> level a part of the excitation is transferred to the <sup>5</sup>I<sub>7</sub> level by a phonon deexcitation process. The cross relaxation process ending on the <sup>5</sup>I<sub>6</sub> level creates in connection with ESA2 an avalanche mechanism similar to the case

of  $\text{Ho}^{3+}$ ,  $\text{Yb}^{3+}:\text{YAIO}_3$ . This process occurs simultaneously with the looping mechanism based on the ESA1. The upconversion processes  $u_1$  and  $u_2$  occur, also reducing the efficiency of the cross-relaxation process.

As we have discussed, in the case of codoping with  $\text{Yb}^{3+}$ , the two cross-relaxation processes  $s$  and  $s_3$  affect the emitting level in comparison with the single  $\text{Ho}^{3+}$ , where only the cross-relaxation  $s$  exists. Because the cross-relaxation process is used to feed back the reservoir level from where the ESA take place, the efficiency of such a mechanism is very important for the total balance of the whole upconversion process.

Green emission was observed in  $\text{Ho}^{3+}$ ,  $\text{Yb}^{3+}:\text{YLF}$  system after excitation in the spectral range of 790–820 nm and in the spectral range of 830–850 nm. In the 830–850 nm excitation case only excited state absorption transitions from the  $^5I_6$  level exist, generating together with the cross relaxation  $s_3$  and the back transfer  $s_4$  the upconverted green emission. The ESA process for the 790–820 nm excitation is attributed to the transition  $^5I_6 \rightarrow ^5F_2$  (ESA3, Fig. 3). The ground state absorption GSA2 ( $^5I_8 \rightarrow ^5I_6$ ) is non-resonant and occurs only phonon-assisted. For the second excitation between 830 nm and 850 nm only the ESA process is different, *i.e.*  $^5I_6 \rightarrow ^5F_3$  (ESA4). The cross-relaxation processes remain the same and the ground state absorption is also non-resonant and occurs only phonon-assisted.

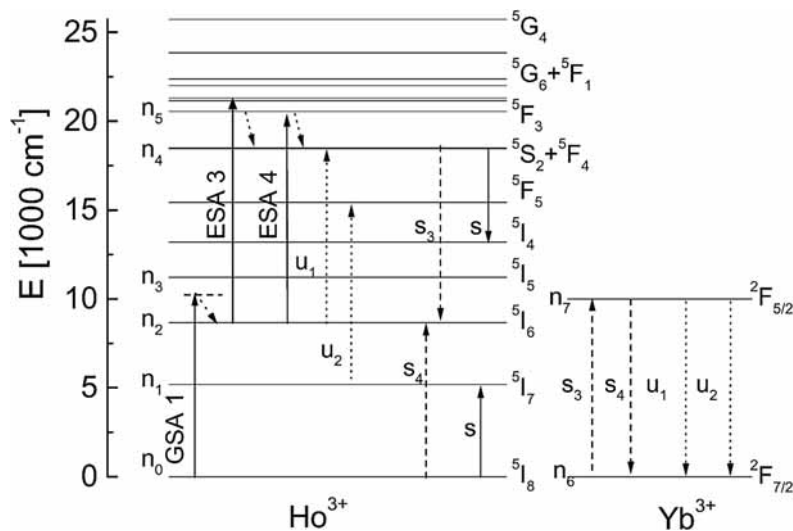


Fig. 3 – Upconversion scheme for  $\text{Ho}^{3+}$ ,  $\text{Yb}^{3+}$  systems under excitation around 800 nm and around 830 nm.

In order to prove the existence of the avalanche mechanism in the Ho-Yb system the temporal evolution of population and the pump power dependence of

the green emission intensity were registered for both 750 nm and 798 nm excitation and are presented in Figs. 4 and 5, respectively. The characteristics of the avalanche process are clearly observed.

Nevertheless a comparison between the efficiency of these processes in samples with and without  $\text{Yb}^{3+}$  cannot be performed without numerical simulations using a system of rate equations.

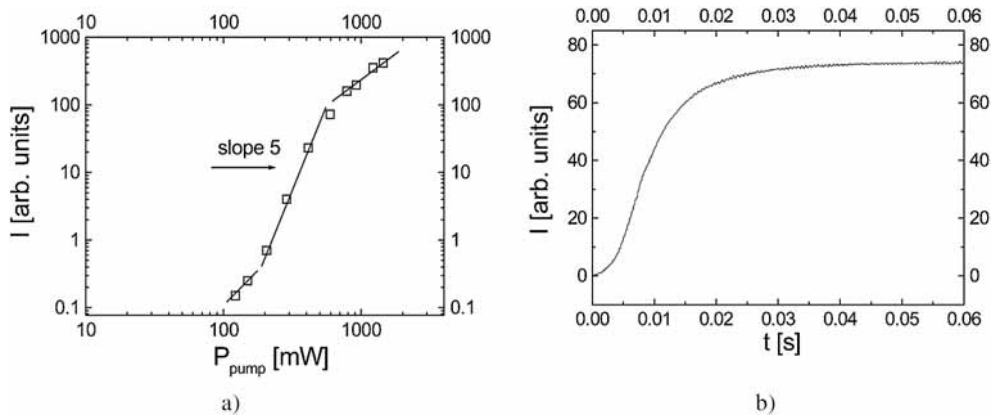


Fig. 4 – Pump power dependence of the green emission (a) and temporal dependence of the green emission (b) for  $\text{Ho}^{3+}$  (1%),  $\text{Yb}^{3+}$ (10%):YLF under 750nm excitation.

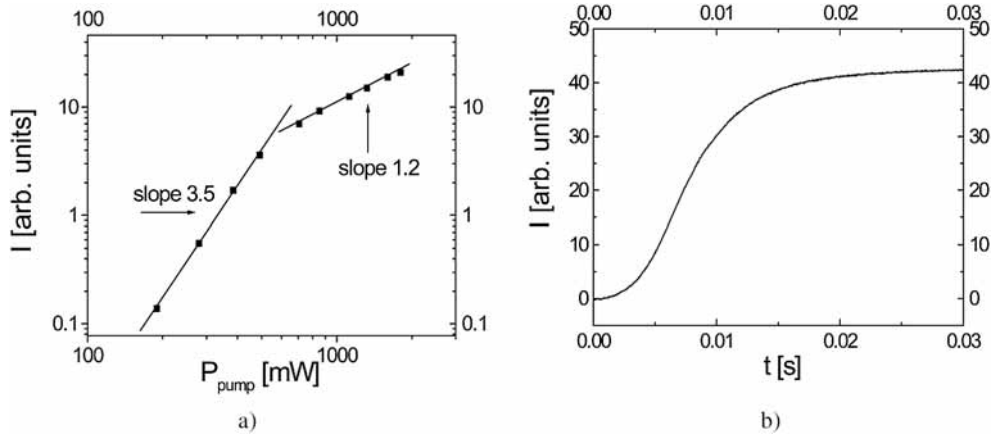


Fig. 5 – Pump power dependence in logarithmic scale (a) and temporal dependence (b) of the green emission for  $\text{Ho}^{3+}, \text{Yb}^{3+}\text{:YLF}$  under 798 nm excitation.

In order to estimate the efficiency of the new energy transfer processes we have performed measurements on the lifetime of the levels involved. Using the results, the transfer rates can be calculated using the following equation:

$$W_{\text{trans}} = W_{\text{tot}} - W,$$

where  $W_{tot}$  and  $W_0$  are the total deexcitation rates in the presence (from the measured decay) and in the absence (intrinsic decay at very low dopant ion concentration) of the transfer process, respectively, and  $W_{trans}$  represents the transfer rate. In fact to determine the transfer rate from  $\text{Ho}^{3+}$  to  $\text{Yb}^{3+}$  we make use of  $W_0$  as the decay for the single doped  $\text{Ho}^{3+}$  sample having the same  $\text{Ho}^{3+}$  concentration as the  $\text{Ho}^{3+}$ ,  $\text{Yb}^{3+}$  sample. Fig. 6a presents the lifetime measurements for the  ${}^5S_2$  level for the two samples used in measurements. For the  $\text{Yb } {}^5F_{7/2}$  level the decays are depicted in Fig. 6b. Because of the nonexponential character of the decays, the rates were calculated using the equation

$$W = \frac{1}{\int_0^{\infty} n(t) dt},$$

where  $n(t)$  is the normalized decay curve.

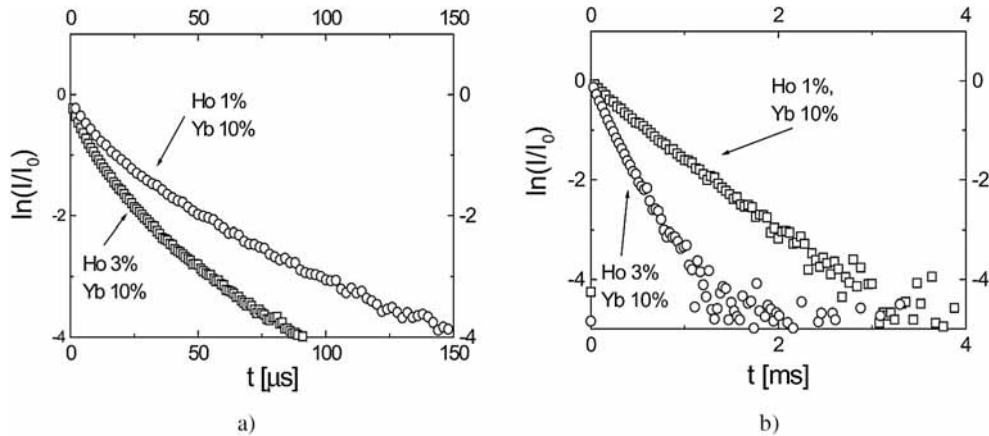


Fig. 6 – Decay measurements in logarithmic scales of the  ${}^5S_2$  ( $\text{Ho}^{3+}$ ) (a) and  ${}^2F_{5/2}$  ( $\text{Yb}^{3+}$ ) (b) level, for  $\text{Ho}^{3+}$  (1%, 3%),  $\text{Yb}^{3+}$  (10%):YLF samples.

The system of rate equation is similar with the system used in [8] to describe the single  $\text{Ho}^{3+}$  system. For the sake of simplicity we only provided here the equations, that should be added in order to describe the interaction between the  $\text{Ho}^{3+}$  and the  $\text{Yb}^{3+}$  ion (as depicted in Fig. 2 and Fig. 3).

$$({}^2F_{7/2}): \frac{dn_{10}}{dt} = -\frac{dn_{11}}{dt},$$

$$({}^2F_{5/2}): \frac{dn_{11}}{dt} = -w_{11} * n_{11} + s_3 * n_{10} * n_6 - s_4 * n_{11} * n_0 - u_1 * n_{11} * n_2 - u_2 * n_{11} * n_1,$$

$$n^I = n_{10} + n_{11},$$

where  $n_{10}$  and  $n_{11}$  represent the populations of the  ${}^2F_{7/2}$  and  ${}^2F_{5/2}$  levels of the Yb<sup>3+</sup>-ion, respectively,  $n^l$  is the total Yb<sup>3+</sup> concentration,  $s_3$  and  $s_4$  are the cross-relaxation rates ( $({}^5S_2, {}^2F_{7/2}) \rightarrow ({}^5I_6, {}^2F_{5/2})$ ) and ( $({}^5I_8, {}^2F_{5/2}) \rightarrow ({}^5I_6, {}^2F_{7/2})$ ), respectively, and  $u_1$  and  $u_2$  are the upconversion processes ( $({}^5I_6, {}^5F_{5/2}) \rightarrow ({}^5S_2, {}^5F_{7/2})$ ) and ( $({}^5I_7, {}^5F_{5/2}) \rightarrow ({}^5F_5, {}^5F_{7/2})$ ), respectively. Also one should add the following terms to already existing equations, [8, eq. 8]:

- to the eq.  ${}^5I_8$  the following term should be added:  $-s_4 * n_{11} * n_0$ ;
- to the eq.  ${}^5I_7$  the following term should be added:  $-u_2 * n_{11} * n_1$ ;
- to the eq.  ${}^5I_6$  the following term should be added:  $+s_3 * n_{10} * n_6 + s_4 * n_{11} * n_0 - u_1 * n_{11} * n_2$ ;
- to the eq.  ${}^5F_5$  the following term should be added:  $+u_2 * n_{11} * n_1$ ;
- to the eq.  ${}^5S_2 + {}^5F_4$  the following term should be added:  $-s_3 * n_{10} * n_6 + u_1 * n_{11} * n_2$ .

The system of rate equation involves the pumping rates, which can be calculated using the formula  $R = \frac{I * \sigma_{abs}}{S}$ , where  $I$  is the photon flux of the pumping process,  $\sigma_{abs}$  is the absorption cross-section and  $S$  is the spot area of the excitation beam.

The rates  $u_1$  and  $u_2$  were treated as adjustable parameters. The radiative lifetimes for the Ho<sup>3+</sup> and Yb<sup>3+</sup> in YLF were taken from [35, 36].

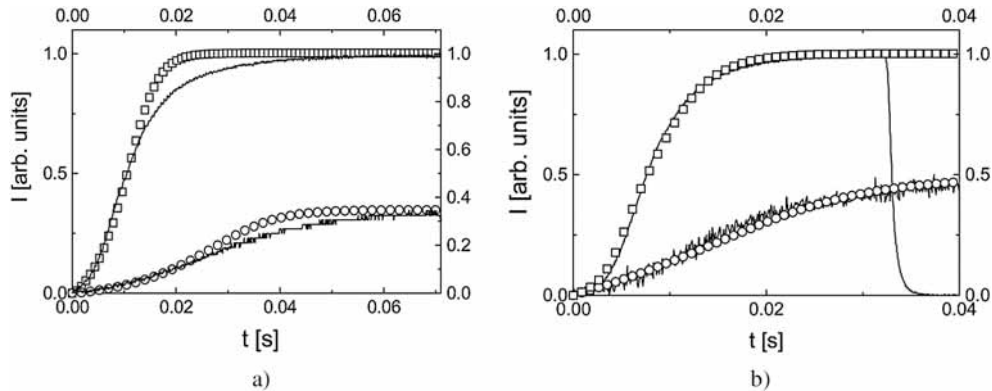


Fig. 7 – a) Measured temporal dependence of the green emission (solid line) under 750 nm excitation in comparison with the calculated temporal dependence of the green emission (open squares for a pump rate above the threshold value and open circles for a pump rate around the threshold value) for the Ho<sup>3+</sup>,Yb<sup>3+</sup>:YLF system; b) measured temporal dependence of the green emission (solid line) under 798 nm excitation in comparison with the calculated temporal dependence of the green emission (open squares for a pump rate above the threshold value and open circles for a pump rate below the threshold value) for the Ho<sup>3+</sup>,Yb<sup>3+</sup>:YLF system.

Using the numerical results the measured temporal dependencies of the upconverted green emission, one above the threshold value and one below the threshold value, were fitted using the same value for the parameters except the values for the pump rates (Figs. 7a and 7b). The only fit parameters were the two transfer rates  $u_1$  and  $u_2$ .

The numerical solutions of the rate equation fit well the experimental results. The position of the Stark levels in order to calculate the Boltzmann factors were taken from [37, 38].

### 3. CONCLUSION

In conclusion we have put into evidence the avalanche mechanism under 750 nm excitation generating green emission in  $\text{Ho}^{3+}, \text{Yb}^{3+} : \text{YLF}$  system. Also the avalanche mechanism under excitation in the 790–850 nm spectral range was demonstrated.

Based on spectroscopic parameters using a system of rate equations a numerical simulation of the upconversion mechanism was performed and the results were compared with the experimentally observed temporal behavior of the green emission. With the help of the rate equation model it was shown that in a  $\text{Ho}^{3+}, \text{Yb}^{3+} : \text{YLF}$  system the avalanche mechanism under 750 nm excitation can be more efficient than in a single  $\text{Ho}^{3+} : \text{YLF}$  system.

### REFERENCES

1. A. V. Kiryanov, V. Aboites, A. M. Belovolov, M. J. Damzen, A. Minassian, M. I. Timoshechkin, M. I. Belovolov, *J. Luminescence*, **102–103**, 715 (2003).
2. J. A. Capobianco, J. C. Boyer, F. Vetrone, A. Speghini, M. Bettinelli, *Chem. of Materials*, **14**, 2915 (2002).
3. A. Wnuk, M. Kaczkan, Z. Frukacz, I. Pracka, G. Chadeyron, M.-F. Joubert, M. Malinowski, *J. Alloys and Compounds*, **341**, 353 (2002).
4. I. Sokólska, *J. Alloys and Compounds*, **341**, 288 (2002).
5. E. Osiac, *J. Alloys and Compounds*, **341**, 263 (2002).
6. P. Deren, A. A. Demidovich, J. C. Krupa, W. Strek, *J. Alloys and Compounds*, **341**, 130 (2002).
7. S. Kück, I. Sokólska, *Chem. Phys. Lett.*, **325**, 257 (2000).
8. E. Osiac, I. Sokólska, S. Kück, *Phys. Rev.*, **B 65**, 235119 (2002).
9. E. Osiac, I. Sokólska, S. Kück, *J. of Luminescence*, **94–95**, 289 (2001).
10. E. Osiac, I. Sokólska, S. Kück, *J. Alloys and Compounds*, **323–324**, 283 (2001).
11. T. Wenyan, B. R. Reddy, *J. of Applied Physics*, **88**, 1221, (2000).
12. M.-F. Joubert, S. Guy, M. Malinowski, R. Piramidowicz, A. Wnuk, G. Chadeyron, *Radiation Effects and Defects in Solids*, **150**, 471 (1999).
13. M. Malinowski, R. Piramidowicz, Z. Frukacz, G. Chadeyron, R. Mahiou, M.-F. Joubert, *Optical Materials*, **12**, 409 (1999).
14. Z. Xiao, J. P. Jouart, G. Mary, *J Phys. Condens. Matt.*, **10**, 493 (1998).

15. F. Lahoz, I. R. Martin, D. Alonso, *Physical Review*, **B 71**, 045115 (2005).
16. X. X. Luo, W. H. Cao, *Material Letters*, **61**, 3696–3700 (2007).
17. M.-F. Joubert, S. Guy, B. Jacquier, *Phys. Rev.*, **B 48**, 10031 (1993).
18. M.-F. Joubert, S. Guy, B. Jacquier, C. Linares, *Optical Materials*, **4**, 43 (1994).
19. R. Scheps, *Progress in Quantum Electronics*, **20**, 4 (1996).
20. J. S. Chivian, W. E. Case, D. D. Eden, *Appl. Phys. Lett.*, **35**, 124 (1979).
21. A. W. Kueny, W. E. Case, M. E. Koch, *J. Opt. Soc. Am.*, **B 6**, 639 (1989).
22. G. Huber, E. Heumann, T. Sandrock, K. Petermann, *J. Luminescence*, **72–74**, 1 (1997).
23. V. Lupei, E. Osiac, T. Sandrock, E. Heumann, G. Huber, *J. Luminescence*, **76**, 441 (1998).
24. H. Ni, S. C. Rand, *Optics Letters*, **16**, 1424 (1991).
25. Q. Shy, H. Ni, S. C. Rand, *Optics Letters*, **22**, 123 (1997).
26. W. Lenth, R. M. Macfarlane, *J. Luminescence*, **45**, 346 (1990).
27. N. Pelletier-Allard, R. Pelletier, *Phys. Rev.*, **B 36**, 4425 (1987).
28. N. J. Krasutsky, *J. Appl. Phys.*, **54**, 1261 (1983).
29. M. Malinowski, R. Piramidowicz, Z. Frukacz, G. Chadeyron, R. Mahiou, M.-F. Joubert, *Optical Materials*, **12**, 409 (1999).
30. S. Kück S, E. Osiac, I. Sokólska, *Journal of the Optical Society of America B - Optical Physics*, **22**, 323 (2005).
31. R. K. Watts, *J. of Chem. Phys.*, **53**, 3552 (1970).
32. M. A. Chamarro, R. Cases, *J. Luminescence*, **42**, 267 (1988).
33. A. Brenier, L. C. Courrol, C. Pedrini, C. Madej, G. Boulon, *Phys. Rev.*, **B 49**, 881 (1994).
34. L. F. Johnson, H. J. Guggenheim, *Appl. Phys Lett.*, **19**, 44 (1971).
34. X. X. Zhang, P. Hong, M. Bass, B. H. T. Chai, *Appl. Phys. Lett.*, **63**, 2606 (1993).
35. A. M. Tkachuk, A. V. Khilko, M. V. Petrov, *Opt. Spektrosk.*, **58**, 91 (1985).
36. L. A. DeLoach, S. A. Payne, L. L. Chase, L. K. Smith, W. L. Kway, W. F. Krupke, *J. Quant. Electr.*, **29**, 1179 (1993).
37. A. A. Kaminskii, *Laser Crystals*, Springer-Verlag, Berlin, 1990, 2nd ed., p 140.
38. S. N. Gifeisman, A. M. Tkachuk, V. V. Prizmak, *Opt. Spektrosk.*, **44**, 120 (1978).